New Mono- and Dinuclear Titanium(III) Complexes. The Crystal Structure of and Exchange Coupling in [{LTi^{III}(NCO)$_2$}$_2$(μ-O)] (L = 1,4,7-Trimethyl-1,4,7-triazacyclononane)

Peter Jeske,† Karl Wieghardt,*,† and Bernhard Nuber‡

Lehrstuhl für Anorganische Chemie I, Ruhr-Universität, D-4630 Bochum, Germany, and the Anorganisch-Chemisches Institut der Universität Heidelberg, Im Neuenheimer Feld 270, D-6900 Heidelberg, Germany

Received July 14, 1993•

Ti^{III}(CH$_3$CN)$_3$Cl$_3$ in acetonitrile solution reacts with the cyclic triamine 1,4,7-triisopropyl-1,4,7-triazacyclononane (tiptacn) with formation of green [(tiptacn)Ti^{III}Cl$_3$] (**1**). The chloro ligands in **1** are readily substituted by thiocyanate generating [(tiptacn)Ti(NCS)$_3$] (**2**). From a mixture of tetrahydrofuran, NaOCN, water, and methanol and **1** the complex [(tiptacn)Ti^{III}(NCO)$_2$(OCH$_3$)] (**3**) was obtained. In the absence of methanol and by using 1,4,7-trimethyl-1,4,7-triazacyclononane (Me$_3$tacn) as macrocyclic triamine, the neutral (μ-oxo)dititanium(III) complex [(Me$_3$tacn)$_2$Ti$_2$ (NCO)$_4$(μ-O)] (**4**) formed. The corresponding thiocyanato analogue [(Me$_3$tacn)$_2$Ti$_2$(NCS)$_4$(μ-O)] (**5**) was obtained from an acetonitrile/water mixture of [(Me$_3$tacn)Ti(NCS)$_3$]. The crystal structure of **4** has been determined by X-ray crystallography: space group *Pbca*, a = 12.532(4) Å, b = 14.379(4) Å, c = 16.366(5) Å, V = 2949.1(20) Å^3, Z = 4. The neutral molecules in **4** contain a linear Ti^{III}–O–Ti^{III} moiety with a Ti–O bond distance of 1.838(1) Å. From temperature dependent magnetic susceptibility measurements (2.0–296 K) it is concluded that the two unpaired electrons in **4** and **5** are weakly intramolecularly antiferromagnetically coupled ($H = -2JS_1 \cdot S_2$; $S_1 = S_2 = {}^1/_2$; **4**, J = −7.8 cm^{-1}; **5**, J = −5.6 cm^{-1}). Electronic and X-band ESR-spectra, the electrochemistry, and the magnetic properties of complexes **1**–**5** have been investigated in detail.

Introduction

The phenomenon of intramolecular spin exchange coupling via σ- or π-superexchange mechanisms has been studied over the past 30 years in considerable detail.[1] Linearly μ-oxo bridged transition metal complexes represent probably the most extensively studied class of compounds in this respect. For numerous (μ-oxo)dichromium(III)[2] and (μ-oxo)diiron(III)[3] species with an octahedral ligand environment strong antiferromagnetic coupling (S = 0 ground state) between the two paramagnetic metal ions with d^3d^3 or high-spin d^5d^5 electronic configuration is well established and theoretically understood (Chart 1). Only recently, Armstrong et al.[4a] have shown that the same magnetic properties prevail in a linear (μ-oxo)dimanganese(III) species with a high-spin d^4d^4 configuration. On the other hand, we and others have discovered that in (μ-oxo)divanadium(III) complexes (d^2d^2) the spins of all four unpaired electrons are aligned—sometimes even at room temperature.[5] Thus very strong *ferromagnetic* spin exchange coupling yielding an S = 2 ground state is experimentally observed for these divanadium(III) complexes. An interpretation of this behavior in the frame of the Goodenough–Kanamori rules for magnetic superexchange[6] has recently been published.[7]

Chart 1. Exchange Coupling in Linear (μ-Oxo)dimetal(III) Complexes

M^{III}	d^n		J,[a] cm^{-1}	ref
Ti	d^1	weakly antiferromagnetic	−7	this work
V	d^2	ferromagnetic	>+200	5
Cr	d^3	antiferromagnetic	−250	2
Mn	d^4 (h.s.)	antiferromagnetic	−120	4
Fe	d^5 (h.s.)	antiferromagnetic	−100	3

[a] $H = -2JS_1 \cdot S_2$ ($S_1 = S_2$).

In the light of these detailed studies it is very surprising that the electronically most simple case involving a first-row transition metal with a d^1 electronic configuration has not been studied experimentally to date. The reason for this gap is due to the synthetic inaccessibility of (μ-oxo)dititanium(III) species. A literature search revealed that only two such complexes have been structurally characterized,[8] namely [{(py)$_3$TiBr$_2$}$_2$(μ-O)] and [{Cp$_2$Ti}$_2$(μ-O)]. In both cases no magnetochemical information has been presented. We have recently synthesized [(Me$_3$tacn)$_2$Ti$_2$Cl$_4$(μ-O)] and measured its magnetic susceptibility in the temperature range 80–298 K and concluded from these measurements that the spins are uncoupled ($H = -2JS_1 \cdot S_2$; $S_1 = S_2 = {}^1/_2$; $J \sim 0$ cm^{-1}).[9] At that time we were only able to grow single crystals suitable for X-ray crystallography of its para-

† Ruhr-Universität.
‡ Universität Heidelberg.
• Abstract published in *Advance ACS Abstracts*, December 1, 1993.

(1) (a) Martin, R. L. In *New Pathways in Inorganic Chemistry*, Ebsworth, E. A., Maddock, J., Sharpe, A. G., Eds.; Cambridge University Press: Cambridge, England, 1968; pp 175. (b) Ginsberg, A. P. *Inorg. Chim. Acta Rev.* **1971**, 45. (c) Sinn, E. *Coord. Chem. Rev.* **1970**, *5*, 313; (d) Kahn, O. *Angew. Chem.* **1985**, *97*, 837; *Angew. Chem., Int. Ed. Engl.* **1985**, *24*, 834. (e) Hay, P. J.; Thibeault, J. C.; Hoffmann, R. *J. Am. Chem. Soc.* **1975**, *97*, 4884.
(2) (a) West, B. O. *Polyhedron* **1989**, *8*, 219. (b) Pedersen, E. *Acta Chem. Scand.* **1972**, *26*, 333. (c) Glerup, J. *Acta Chem. Scand.* **1972**, *26*, 3775. (d) Güdel, H. U.; Dubicki, L. *Chem. Phys.* **1974**, *6*, 272. (e) Schmidtke, H.-H. *Theor. Chim. Acta* **1971**, *20*, 92. (f) McCarthy, P. J.; Güdel, H. U. *Coord. Chem. Rev.* **1988**, *88*, 69.
(3) (a) Murray, K. S. *Coord. Chem. Rev.* **1974**, *12*, 1. (b) Kurtz, D. M., Jr. *Chem. Rev.* **1990**, *90*, 585.
(4) (a) Kipke, C. A.; Scott, M. J.; Gohdes, J. W.; Armstrong, W. H. *Inorg. Chem.* **1990**, *29*, 2193. (b) Kitajima, N.; Osawa, M.; Tanaka, M.; Moro-oka, Y. *J. Am. Chem. Soc.* **1991**, *113*, 8952.
(5) (a) Knopp, P.; Wieghardt, K.; Nuber, B.; Weiss, J.; Sheldrick, W. S. *Inorg. Chem.* **1990**, *29*, 363. (b) Money, J. K.; Folting, K.; Huffman, J. C.; Christou, G. *Inorg. Chem.* **1987**, *26*, 944. (c) Brand, S. G.; Edelstein, N.; Hawkins, C. J.; Shalimoff, G.; Snow, M. R.; Tiekink, E. R. T. *Inorg. Chem.* **1990**, *29*, 434.
(6) (a) Goodenough, J. B. *Magnetism and the Chemical Bond*; Wiley-Interscience: New York, 1976. (b) Kanamori, J. *J. Phys. Chem.* **1959**, *10*, 87; (c) Anderson, P. W. In *Solid State Physics*; Seitz, F.; Turnbull, D., Ed.; Academic Press: New York, 1963; Vol. 14.
(7) Hotzelmann, R.; Wieghardt, K.; Flörke, U.; Haupt, H.-J.; Weatherburn, D. C.; Bonvoisin, J.; Blondin, G.; Girerd, J.-J. *J. Am. Chem. Soc.* **1992**, *114*, 1681.
(8) (a) Troyanov, S. I.; Mazo, G. N.; Rybakov, V. B.; Budkina, K. V. *Koord. Khim.* **1990**, *16*, 466. (b) Honold, B.; Thewalt, U.; Herberhold, M.; Alt, H. G.; Kool, L. B.; Rausch, M. D. *J. Organomet. Chem.* **1986**, *314*, 105.
(9) (a) Bodner, A.; Della Vedova, B. S. P. C.; Wieghardt, K.; Nuber, B.; Weiss, J. *J. Chem. Soc., Chem. Commun.* **1990**, 1042. (b) Bodner, A.; Jeske, P.; Weyhermüller, T.; Wieghardt, K.; Dubler, E.; Schmalle, H.; Nuber, B. *Inorg. Chem.* **1992**, *31*, 3737.

0020-1669/94/1333-0047$04.50/0

magnetic mixed valence form $[(Me_3tacn)_2Ti_2Cl_4(\mu\text{-}O)]Cl\cdot 2H_2O$ which contains a linear Ti^{III}–O–Ti^{IV} group.[9]

Here we report the synthesis, spectroscopic characterization, electrochemistry, and magnetic properties of a series of mononuclear titanium(III) complexes $[(tiptacn)TiX_3]$ containing the bulky macrocyclic triamine 1,4,7-triisopropyl-1,4,7-triazacyclononane. Furthermore, the two (μ-oxo)dititanium(III) complexes $[(Me_3tacn)_2Ti_2(NCO)_4(\mu\text{-}O)]$ (**4**) and $[(Me_3tacn)_2Ti_2(NCS)_4(\mu\text{-}O)]$ (**5**) have been synthesized. Complex **4** has been structurally characterized by X-ray crystallography; the magnetic properties of **4** and **5** are reported, and a model for the intramolecular exchange coupling is presented.

Experimental Section

Reagents. The ligand 1,4,7-triisopropyl-1,4,7-triazacyclononane (tiptacn)[10] and the complex $[(Me_3tacn)Ti(NCS)_3]$[9b] where Me_3tacn represents 1,4,7-trimethyl-1,4,7-triazacyclononane were synthesized according to published procedures.

[(tiptacn)TiCl$_3$] (1). A suspension of $TiCl_3$ (2.8 g, 18 mmol) in deoxygenated CH_3CN (60 mL) was heated to reflux under an argon atmosphere until a clear deep blue solution was obtained from which upon cooling to room temperature blue microcrystals of $Ti(CH_3CN)_3Cl_3$ precipitated. To this mixture was added the deoxygenated ligand tiptacn (6.0 g, 24 mmol). Heating to 40 °C initiated the formation of a green-brown solution from which within 1 h green microcrystals precipitated which were filtered off, washed with water, acetonitrile, and finally with diethyl ether, and air-dried. The solid material is stable in air and is not particularly hygroscopic. Yield: 5.4 g (73%). Anal. Calcd for $C_{15}H_{33}N_3Cl_3Ti$: C, 44.0; H, 8.1; N, 10.3. Found: C, 43.9; H, 8.2; N, 10.2.

[(tiptacn)Ti(NCS)$_3$] (2). To a mixture of **1** (0.41 g, 1.0 mmol) in deoxygenated tetrahydrofuran (10 mL) and water (10 mL) was added NaSCN (0.81 g, 10 mmol). Stirring under an argon atmosphere for 3 h produced a blue suspension. The green precipitate was filtered off under argon, washed with deoxygenated H_2O, acetone, and diethyl ether and dried in an argon stream. The product was recrystallized from a saturated CH_3CN solution. Yield: 0.28 g (58%). Anal. Calcd for $C_{18}H_{33}N_6S_3Ti$: C, 45.3; H, 6.9; N, 17.6; S, 20.1. Found: C, 45.1; H, 7.0; N, 17.4; S, 20.2.

[(tiptacn)Ti(NCO)$_2$(OCH$_3$)] (3). A deoxygenated reaction mixture consisting of **1** (0.41 g, 1.0 mmol) and NaOCN (0.50 g, 7.7 mmol) in tetrahydrofuran (10 mL), water (15 mL), and methanol (3 mL) was carefully warmed up to 50 °C under an argon atmosphere. After 2–3 h at this temperature the color had changed from green to purple. The resulting purple precipitate was collected by filtration under argon, washed with water, acetone, and diethyl ether, and dried in an argon atmosphere. The product was recrystallized from a saturated CH_3CN solution. Yield: 0.27 g (65%). Anal. Calcd for $C_{18}H_{36}N_5O_3Ti$: C, 51.6; H, 8.6; N, 16.7. Found: C, 51.4; H, 8.9; N, 16.4.

[(Me$_3$tacn)$_2$Ti$_2$(NCO)$_4$(μ-O)] (4). To a deoxygenated solution of NaOCN (1.5 g, 23 mmol) in a tetrahydrofuran/water mixture (1:1, 40 mL) was added $[(Me_3tacn)TiCl_3]$[9b] (1.0 g, 3.1 mmol) at room temperature with stirring. The mixture was heated to reflux under an argon atmosphere for 2 h until a clear purple solution was obtained. When the solution was cooled to 20 °C, a purple precipitate formed which was collected by filtration under argon, washed with deoxygenated H_2O, CH_3CN, and diethyl ether, and dried. The resulting solid is very air-sensitive. Crystals suitable for X-ray crystallography were obtained by Soxhlet extraction of the solid material with refluxing acetonitrile. The extraction procedure was carried out until the precipitation of crystals from the boiling CH_3CN solution started. Slow cooling to 20 °C allowed the precipitation of crystalline **4**. The dry crystalline solid is stable in air for a few days. Yield: 0.84 g (90%). Anal. Calcd for $C_{22}H_{42}N_{10}O_5Ti_2$: C, 42.4; H, 6.8; N, 22.5. Found: C, 42.1; H, 6.8; N, 22.1.

[(Me$_3$tacn)$_2$(NCS)$_4$Ti$_2$(μ-O)] (5). To a deoxygenated solution of $[(Me_3tacn)Ti(NCS)_3]$[9b] (1.0 g, 2.6 mmol) in a mixture of tetrahydrofuran (30 mL) and water (30 mL) was added deoxygenated triethylamine (0.2 mL). The solution was kept in a sealed reaction vessel under an argon atmosphere at ambient temperature for 7 d after which time large, irregularly shaped purple-black crystals precipitated, which were collected by filtration, washed with CH_3CN, and dried under an argon atmosphere. Yield: 0.80 g (90%). Anal. Calcd for $C_{22}H_{42}N_{10}OS_4Ti_2$: C, 38.5; H, 6.1; N, 20.4; S, 18.7. Found: C, 38.3; H, 6.2; N, 20.2; S, 17.9.

Table 1. Crystallographic Data for $[(Me_3tacn)_2Ti_2(NCO)_4(\mu\text{-}O)]$

chem formula	$C_{22}H_{42}N_{10}O_5Ti_2$	fw	622.4
a, Å	12.532(4)	space group	*Pbca* (No. 61)
b, Å	14.379(4)	T, K	298
c, Å	16.366(5)	λ, Å	0.710 73
V, Å^3	2949.1(20)	ρ_{calcd}, g·cm^{-3}	1.40
Z	4	μ, mm^{-1}	0.58
R^a	0.066 (obsd data)	$R_w{}^b$	0.066 (obsd data)

^{a} $R = \sum||F_o|-|F_c||/\sum|F_o|$. ^{b} $R_w = \{\sum w(F_o-F_c)^2/\geq w|F_o|^2\}^{1/2}$; $w = 1/(\sigma^2(F) + 0.0004F^2)$.

Table 2. Electronic Spectral[a] and Infrared Data for Complexes 1–5

complex	λ_{max}, nm (ϵ, L mol^{-1} cm^{-1})	IR,[b] cm^{-1}	assignment
1	734 (28), 264 (3700), 227 (5100)		
2	596 (32), 346 (1.1 × 10^4), 309 (1.3 × 10^4), 275 (2.3 × 10^4), 242 (2.1 × 10^4)	493 (w)	δ(NCS)
		2059 (vs), 2017 (vs)	ν(NCS)
3	685 (13), 533 (16), 270 (2.0 × 10^4)	2211 (vs), 2188 (vs)	ν(NCO)
		627 (w), 607 (w)	δ(NCO)
		2807 (vw)	$\nu_{CH}(OCH_3)$
		1124 (w)	$\nu_{CO}(OCH_3)$
		573 (w)	$\nu_{TiO}(OCH_3)$
4	665 (30), 535 (45), 235 (1.0 × 10^4)	2192 (vs)	ν(NCO)
		631 (w)	δ(NCO)
		748 (s)	ν(Ti–O–Ti)
5	615 (48), 504 (67), 275 (3.2 × 10^3)	2045 (vs)	ν(NCS)
		485 (w)	δ(NCS)
		739 (s)	ν(Ti–O–Ti)

^{a} Solvent: CH_3CN. ^{b} vs = very strong; s = strong; w = weak; KBr disks.

Physical Measurements. The apparatus used for cyclic voltammetric and coulometric measurements has been described previously.[11] Cyclic voltammograms were recorded in CH_3CN solutions containing 0.10 M tetra-*n*-butylammonium hexafluorophosphate as supporting electrolyte ([complex] ~ 10^{-3} M). A glassy-carbon working electrode, a Pt-wire auxilliary electrode, and a Ag/AgCl (saturated LiCl in ethanol) reference electrode were used throughout.

Magnetic susceptibilities of powdered samples were measured by using a SQUID magnetometer (Quantum design) in the temperature range 2.0–295 K. Corrections for underlying diamagnetism were applied with use of Pascal's constants. X-band ESR spectra of solid samples were recorded on a Bruker ER 200 spectrometer; electronic absorption spectra were measured on a Perkin-Elmer Lambda 9 spectrophotometer; infrared spectra were recorded as KBr disks on a Perkin-Elmer FT-IR spectrometer Model 1720 X.

X-ray Structure Determination. Intensities and lattice parameters of a purple plate shaped crystal of **4** were measured on a Syntex R3 diffractometer at ambient temperature by using graphite-monochromated Mo Kα X-radiation. Crystal parameter and details of the data collection are given in Table 1. An empirical absorption correction (ψ-scans of seven reflections with $7.0 \leq 2\vartheta \geq 39°$) was carried out. The structure was solved with conventional Patterson and difference Fourier methods.[12] The function minimized during full-matrix least-squares refinement was $\sum w(|F_o|-|F_d|)^2$, where $w = 1/(\sigma(F)^2 + 0.0004F_o^2)$. Neutral atom scattering factors and anomalous dispersion corrections were taken from ref 13. The positions of H-atoms were calculated (C–H = 0.96 Å) and included in the refinement with a common isotropic thermal parameter $U = 0.080$ Å^2. All other atoms were refined with anisotropic thermal parameters. Final atom coordinates are given in Table 2.

Results

Synthesis and Characterization of Complexes. Scheme 1 summarizes the synthetic results of this work and Table 2 gives

(10) Haselhorst, G.; Stötzel, S.; Strassburger, A.; Walz, W.; Wieghardt, K.; Nuber, B. *J. Chem. Soc., Dalton Trans.* **1993**, 83.

(11) Köppen, M.; Fresen, G.; Wieghardt, K.; Llusar, R. M.; Nuber, B.; Weiss, J. *Inorg. Chem.* **1988**, *27*, 721.

(12) Full-matrix least-squares refinement was performed using the Siemens program package SHELXTL-PLUS (PC-version 1993) (Sheldrick, G. M., University of Göttingen).

(13) *International Tables for X-ray Crystallography*; Kynoch: Birmingham, England, 1974; Vol. IV, pp 99, 149.

Scheme 1. Synthesis of Complexes

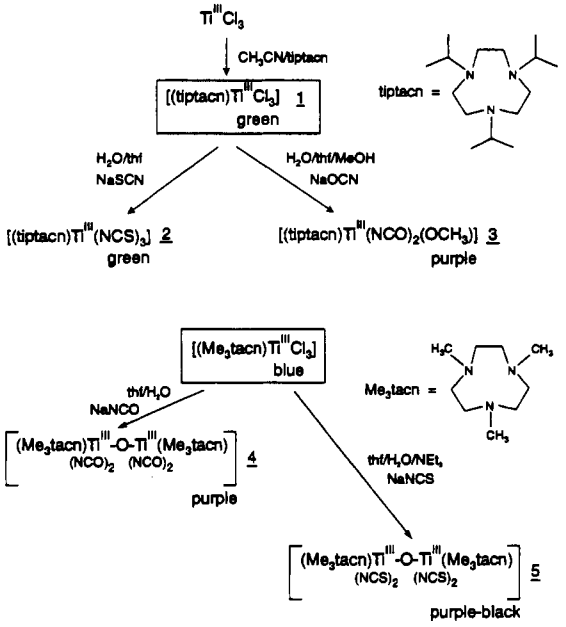

electronic spectral and infrared data for new complexes. The macrocyclic triamine 1,4,7-triisopropyl-1,4,7-triazacyclononane[10] binds strongly to titanium(III) in acetonitrile solutions of $TiCl_3$ under anaerobic conditions with formation of green [(tiptacn)-$TiCl_3$] (**1**). In complex **1** the chloride ligands are readily substituted by thiocyanate in a tetrahydrofuran/water mixture generating green microcrystalline [(tiptacn)$Ti^{III}(NCS)_3$] (**2**). When the same reaction was carried out in the presence of a small amount of methanol and by using sodium cyanate instead of thiocyanate, purple microcrystals of [(tiptacn)$Ti^{III}(NCO)_2$-(OCH_3)] (**3**) were obtained in good yields. Complexes **1–3** are fairly stable toward oxygen and water in the solid state but are very unstable in solution. Dinuclear species containing the linear Ti^{III}–O–Ti^{III} entity were prepared by hydrolysis of [(Me_3tacn)-$TiCl_3$][9b] in a tetrahydrofuran/water mixture (1:1) under anaerobic conditions in the presence of NaNCO yielding [(Me_3-tacn)$_2Ti^{III}_2(NCO)_4(\mu$-O)] (**4**) or NaNCS with formation of [(Me_3tacn)$_2Ti^{III}_2(NCS)_4(\mu$-O)] (**5**). Microcrystalline purple **4** and **5** are only moderately air-sensitive in the solid state but very in solution. For complexes **2–5**, the infrared data and the crystal structure determination of **4** establish N-coordination of the cyanate and thiocyanate ligands. Since the macrocyclic ligands tiptacn and Me_3tacn are facially coordinated, the monodentate ligands in **1–3** are also facially bound to the titanium(III) ions. Thus, considering the N_3TiX_2Y coordination spheres only, the symmetry is C_{3v} for **1** and **2** and C_s for **3**.

Figure 1 displays the electronic spectra of **2–4** in acetonitrile solution in the visible region. The electronic spectra of **1** and **2** with idealized C_{3v} symmetry exhibit one slightly asymmetric absorption maximum in the visible which is composed of two transitions of similar energy. Due to a dynamic Jahn–Teller effect a small tetragonal distortion leads to a splitting of the $^2T_2$ ground state and the ^2E first excited state in O_h symmetry into B_2, ^2E and $^2B_1$, $^2A_1$ states, respectively, in a tetragonal ligand field. The transitions $^2B_2 \rightarrow {}^2A_1$ and $^2B_2 \rightarrow {}^2B_1$ are observed. The energy difference between these transitions is larger in complexes **3–5** ($\Delta E > 3500$ cm^{-1}) which is a consequence of the stronger π-donor ligands CH_3O^- and O^{2-} in these species with short Ti–O bonds. It is noted that the spectra of **3** and **4** are very similar in the visible region. This is a clear indication that exchange coupling in the dinuclear species **4** and **5** is small which is in contrast to the electronic spectra of complexes with linear Cr^{III}–O–Cr^{III} moieties as Güdel et al. have discussed in detail.[2f]

X-Band ESR spectra of crystalline samples of **1–4** have been measured at 4.2 and 10 K. Complexes **1** and **2** display rhombic

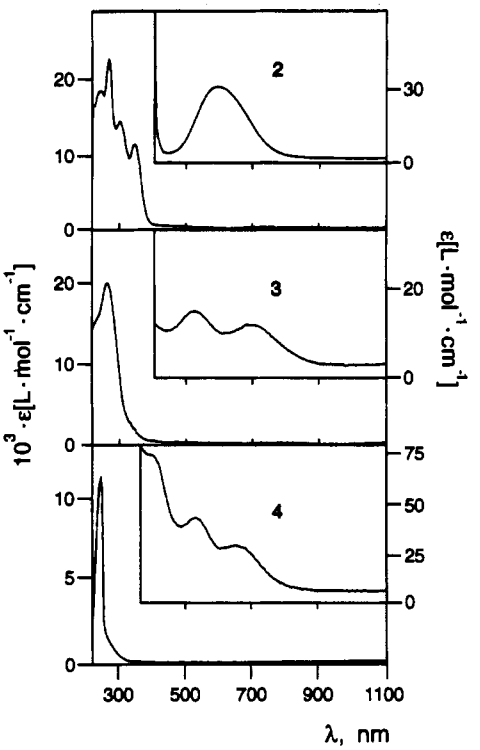

Figure 1. Electronic spectra of mononuclear **2**, **3** and **4** in the visible (CH_3CN solution). Extinction coefficients are per Ti for **2** and **3** and per dinuclear unit for **4**.

Table 3. X-Band ESR Spectra of Crystalline Samples of Complexes

complex	signal	T, K	g values
1	rhombic[a]	4.2	1.50, 1.40
2	rhombic[a]	4.2	1.77, 1.64
3	axial	10	1.95, 1.93

[a] The third g-value at $g_3 < 1.4$ has not been detected unequivocally.

signals and **3** displays an axial signal (Table 3) at $g \sim 2.0$ in accord with the $S = {}^1/_2$ ground state of these complexes. Figure 2 shows the X-band ESR spectrum of **4** at 4.2, 10, 20 and 40 K. At 4.2 K only a very weak isotropic signal at $g = 1.97$ is observed which is due to a small mononuclear impurity with $S = {}^1/_2$ or—most probably—a small amount of the oxidized mixed-valent form of **4**. With increasing temperature the intensity of a signal at $g = 1.98$ increases until it reaches a maximum at ~15 K. At temperatures >10 K a weak low-field signal at 170 mT ($g \sim 4.1$) and one at 450 mT ($g \sim 1.6$) are also detected, both of which are not present at 4.2 K. This is an indication that **4** has a diamagnetic ground state ($S = 0$) with an energetically low-lying first excited state with $S = 1$. From temperature-dependent magnetic susceptibility measurements the energy difference is calculated to be 15.6 cm^{-1} (vide infra). Thus ESR spectroscopy provides evidence for a small antiferromagnetic coupling in **4**.

Magnetic Properties of Complexes. Temperature-dependent magnetic susceptibilities of solid samples of **1–5** have been measured by using a SQUID magnetometer in the range 2.0–295 K. The magnetic moments are given in Table 4. Figure 3 shows the temperature dependence of the magnetic moments and the molar magnetic susceptibilities of the mononuclear complexes **1–3** whereas Figure 4 displays these data for the dinuclear species **4** and **5**. Finally, Figure 5 compares the temperature dependence of the effective magnetic moments per titanium(III) ion of mono- and dinuclear **3** and **4**.

Experimentally, a monotonic decrease of the effective magnetic moments with decreasing temperature is observed for the mononuclear species **1–3** (Table 4). A titanium(III) ion (d^1) in an octahedral ligand field possesses a $^2T_2$ ground state which gives rise to a sizable spin–orbit magnetic momentum and spin–

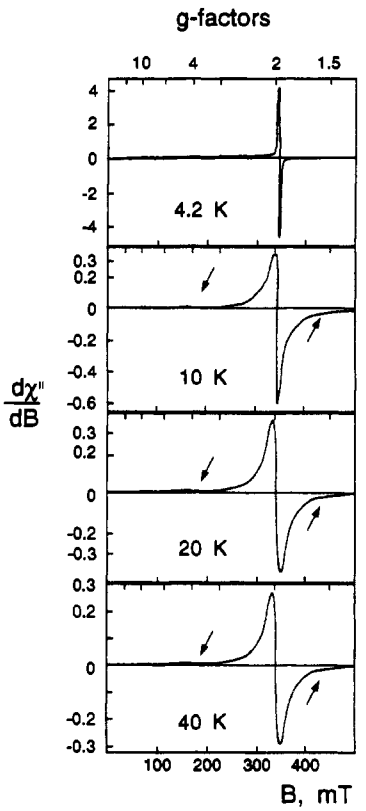

Figure 2. X-band ESR-spectra of crystalline **4** at various temperatures (microwave 9.434 GHz; $\mu W/dB = 20/40$). The arrows mark weak signals at $g \sim 4$ and $g \sim 1.5$.

Table 4. Magnetic Properties of Complexes

complex	μ_{eff}(10 K),[a] μ_B	μ_{eff}(295 K),[a] μ_B	J,[b] cm^{-1}
1	1.26	1.925	
2	1.25	1.68	
3	1.445	1.84	
4	1.05	1.74	−7.8
5	1.12	1.62	−5.6
$(Me_3tacn)TiBr_3$	1.25	1.76	

[a] Calculated per titanium(III) ion. [b] $H = -2JS_1 \cdot S_2$; $S_1 = S_2 = {}^1/_2$.

orbit coupling contributes significantly to the observed magnetic moment of octahedral Ti(III) complexes. Boudreaux and Mulay[14] have calculated the effective magnetic moment by using the spin–orbit coupling constant, ζ, for the free Ti(III) ion of 155 cm^{-1} which predicts a monotonic decrease of μ_{eff} from $\sim 1.9\ \mu_B$ at 300 K to $\sim 0.2\ \mu_B$ at 4 K. The experimentally observed magnetic moments vary considerably less with temperature than is predicted by the Boudreaux and Mulay equation. This is due to orbital momentum quenching by (i) the lower symmetry of the ligand field in complexes **1**–**3** and (ii) to an increasing covalent character of the titanium(III)–ligand bonds and (iii) vibronic mixing of electronic states by nuclear displacements (Ham effect). Effect ii is clearly effective as is deduced by comparing the temperature-dependence of μ_{eff} of **1** and **2** which have the same symmetry, but the Ti–NCS bonds are more covalent than the Ti–Cl bonds. Complex **3** has the lowest symmetry of the present series and strongly covalently bound cyanate and a methoxo ligand. Thus the temperature dependence of the magnetic moment of **3** is the smallest in the mononuclear series. It is important to notice that the susceptibility measurements of mononuclear **1**–**3** do not indicate any *intermolecular* exchange coupling effects. The three bulky isopropyl substituents of the coordinated macrocycle obviously prevent such interactions in the solid state. These results are in agreement with the ESR measurements at 4.2 K which clearly show the $S\ {}^1/_2$ ground state.

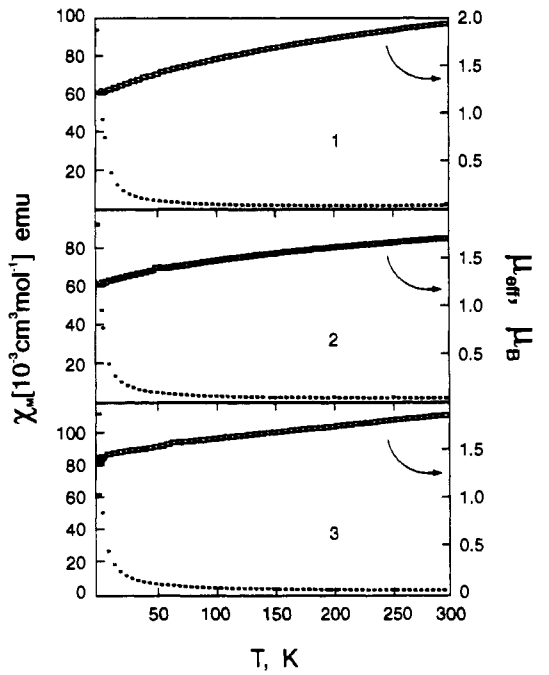

Figure 3. Temperature-dependence of the effective magnetic moments μ_{eff}, and of the molar magnetic susceptibilities, χ_M, of solid samples of **1**, **2**, and **3** (top to bottom).

Table 5. Electrochemical Data[a] of Complexes

complex	$E_{1/2}$, V vs Ag/AgCl	E_{red}, V vs Ag/AgCl	ref
1	+0.48 r	−1.48 irr	this work
2	+0.58 r	−1.18 irr, −1.78 irr	this work
3	−0.21 r	−1.74 irr	this work
$(Me_3tacn)TiBr_3$	+0.53 r	−1.36 irr, −1.58 irr	this work
$(Me_3tacn)TiCl_3$	+0.37 r		9b
$(Me_3tacn)Ti(NCS)_3$	+0.50 r, −1.32 r		9b
4	+0.21 r, −0.55 r		this work
$[(Me_3tacn)_2Ti_2Cl_4(\mu\text{-}O)]$	+0.52 r, −0.38 r		9a, 9b

[a] Conditions: 0.1 M $[TBA]PF_6$ acetonitrile solution; glassy carbon working electrode; Ag/AgCl (saturated LiCl in EtOH) reference electrode; potential range −2.0 to +2.0 V vs Ag/AgCl; scan rate 50 mV s^{-1} r = reversible; irr = ireversible.

The temperature-dependence of the magnetic moment of the dinuclear species **4** and **5** resembles closely that described for the mononuclear complexes in the temperature range 30–295 K (Figure 4). This is demonstrated in Figure 5 where the effective magnetic moments per Ti(III) are plotted vs the temperature for mononuclear **3** and dinuclear **4**. Only below 30 K is a marked decrease of μ_{eff} observed for **4** and **5**, yielding a diamagnetic ground state ($S = 0$) in accord with the ESR measurements. Thus weak intramolecular antiferromagnetic exchange coupling prevails in **4** and **5**.

A least-squares fit to the data using the isotropic Heisenberg model with the Hamiltonian $H = -2JS_1 \cdot S_2$, $S_1 = S_2 = {}^1/_2$, where J and the g value were the only variables, yielded numerical values of $J = -7.8$ cm^{-1} ($g = 1.98$) for **4** and $J = -5.6$ cm^{-1} ($g = 1.85$) for **5**. This model fits the data in the temperature range 2–100 K very well. These absolute J values should not be taken too seriously since the above model does not include spin–orbit coupling, but weak intramolecular antiferromagnetic coupling undoubtedly is experimentally observed. We rule out appreciable intermolecular coupling because this has not been observed for the mononuclear species including $[(Me_3tacn)TiBr_3]$ for which the temperature dependence of μ_{eff} is nearly identical with that of **1**.

(14) Boudreaux, E. A.; Mulay, L. N. *Theory and Application of Molecular Paramagnetism*, Wiley: New York, 1976.
(15) Niemann, A.; Nuber, B.; Wieghardt, K. Unpublished results.
(16) Wieghardt, K.; Pohl, K.; Bossek, U.; Nuber, B.; Weiss, J. *Z. Naturforsch.* **1988**, *43B*, 1184.
(17) Toftlund, H.; Larsen, S.; Murray, K. S. *Inorg. Chem.* **1991**, *30*, 3964.

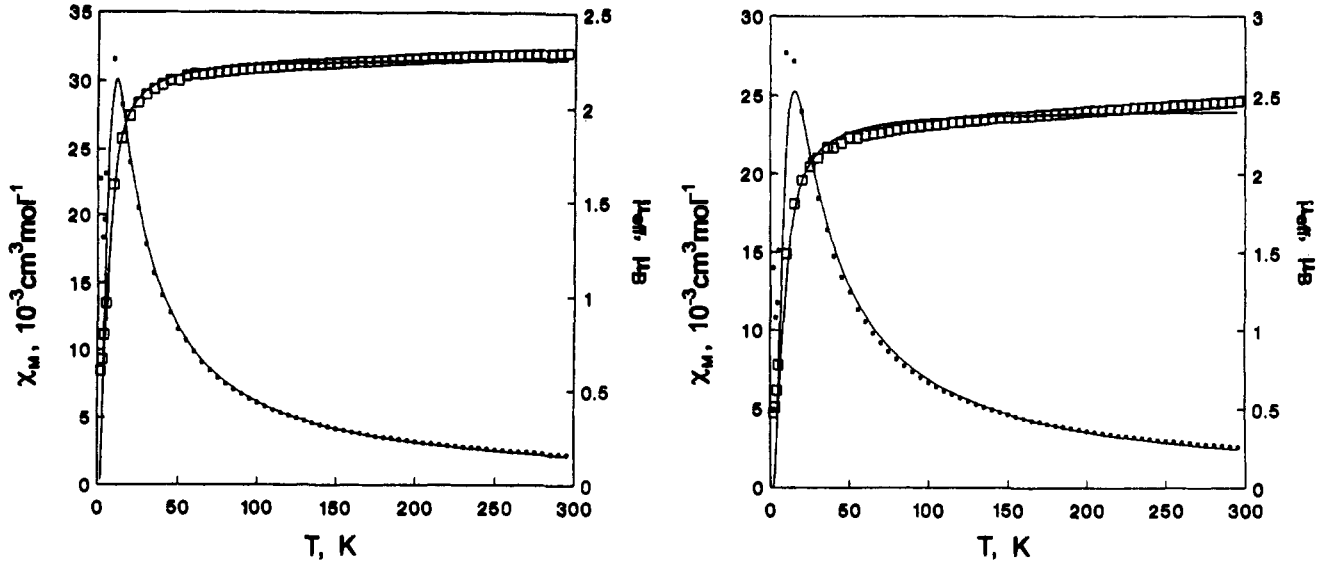

Figure 4. Temperature-dependence of the effective magnetic moments, μ_{eff}, and the molar magnetic susceptibilities, χ_M, of solid samples of the dinuclear species **4** (left) and **5** (right hand side). The solid lines represent best fits using the Hamiltonian $H = -2JS_1 \cdot S_2$ ($S_1 = S_2 = {}^1/_2$) (see text).

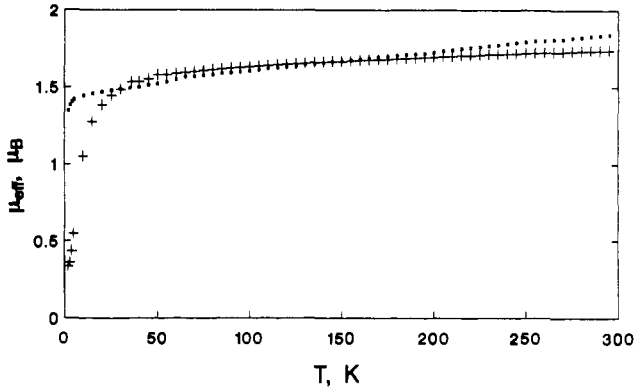

Figure 5. Comparison of the temperature-dependence of the effective magnetic moment per titanium(III) ion of mononuclear **3** (·) and dinuclear **4** (+).

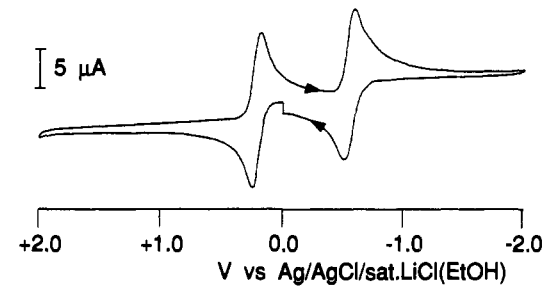

Figure 6. Cyclic voltammogram of **4** in CH_3CN (0.10 M $[TBA]PF_6$) at a glassy-carbon disk electrode at a scan rate of 50 mV s^{-1}.

Electrochemistry. Cyclic voltammograms of complexes **1–5** have been recorded in acetonitrile solution containing 0.10 M tetra-*n*-butylammonium hexafluorophosphate as supporting electrolyte at a glassy-carbon working electrode and a Ag/AgCl (saturated LiCl in ethanol) reference electrode in the potential range −2.0 to +2.0 V vs Ag/AgCl at scan rates 50–200 mV s^{-1}. The results are summarized in Table 5.

The mononuclear species **1–3** show a reversible one-electron oxidation wave, eq 1, which corresponds to the formation of the corresponding Ti(IV) species. The presence of a strong π-donor

$$[(\text{tiptacn})\text{Ti}^{\text{IV}}\text{X}_2\text{Y}]^+ + e^- \rightleftarrows [(\text{tiptacn})\text{Ti}^{\text{III}}\text{X}_2\text{Y}]^0 \quad (1)$$

such as a methoxo ligand in **3** stabilizes the +IV oxidation state by 700–800 mV. A comparison of the redox potentials of **1** and **2** with those of the analogous complexes containing a Me_3tacn ligand reveals that the ligand tiptacn stabilizes the +III oxidation state by 80–110 mV. The reason is unclear.

In addition, species **1–3** display an irreversible one-electron reduction peak at very negative potentials, which is assigned to the formation of unstable Ti(II) species.

The cyclic voltammogram of **4** is shown in Figure 6. Two reversible one-electron transfer waves are observed. Coulometric measurements show that **4** is oxidized by two consecutive one-electron steps generating the relatively stable mixed valent Ti^{III}-Ti^{IV} and Ti^{IV}_2 species eq 2. The electrochemistry of **4** closely resembles that of $[(Me_3tacn)_2Ti^{III}_2Cl_4(\mu\text{-O})]$ where the Ti^{III}_2, the mixed-valent $Ti^{III}Ti^{IV}$, and the colorless Ti^{IV}_2 forms have been isolated as crystalline solids.[9]

$$\mathbf{4} \overset{-e^-}{\underset{+e^-}{\rightleftarrows}} [(Me_3tacn)_2Ti^{3.5}_2(NCO)_4(\mu\text{-O})]^+ \overset{-e^-}{\underset{+e^-}{\rightleftarrows}} [(Me_3tacn)_2Ti^{IV}_2(NCO)_4(\mu\text{-O})]^{2+} \quad (2)$$

The electronic spectrum of the electrochemically generated mixed valent form of **4**, namely $[(Me_3tacn)_2Ti_2(NCO)_4(\mu\text{-O})]^+$, shows three absorption maxima in the visible at 565, 680, and 900 nm as a shoulder. The intensities of these absorptions are quite remarkable with 530, 490, and 200 L mol^{-1} cm^{-1}, respectively, which for the first two is more intense by about 1 order of magnitude as compared to its parent Ti(III) complex **4**. The band at 900 nm is not observed in the spectrum of **4** and is therefore tentatively assigned to an intervalence transition. Attempts to isolate a crystalline salt of the mixed-valent form of **4** failed.

The cyclic voltammogram of **5** shows only two irreversible oxidation waves at anodically shifted potentials as compared to **4**. Upon one-electron oxidation of **5** the oxo bridge is cleaved, and probably two mononuclear species are formed, $[(Me_3tacn)\text{-}Ti^{IV}(O)(NCS)_2]$ and $[(Me_3tacn)Ti^{III}(NCS)_2(CH_3CN)]^+$. The former has been isolated from such solutions and characterized by X-ray crystallography[9b] as a mononuclear six-coordinate titanyl complex.

X-ray Structure of 4. Crystals of **4** consist of well-separated dinuclear neutral molecules $[\{LTi(NCO)_2\}_2(\mu\text{-O})]$. Figure 7 shows the structure, Table 6 gives atom coordinates, and Table 7 summarizes important bond distances and angles. The neutral molecule possesses crystallographically imposed centrosymmetry where the bridging oxygen lies on a crystallographic inversion center. The Ti–O–Ti moiety is therefore linear. Each titanium ion is in a pseudooctahedral environment comprising a facially coordinated triamine, two N-bound monodentate cyanate ligands,

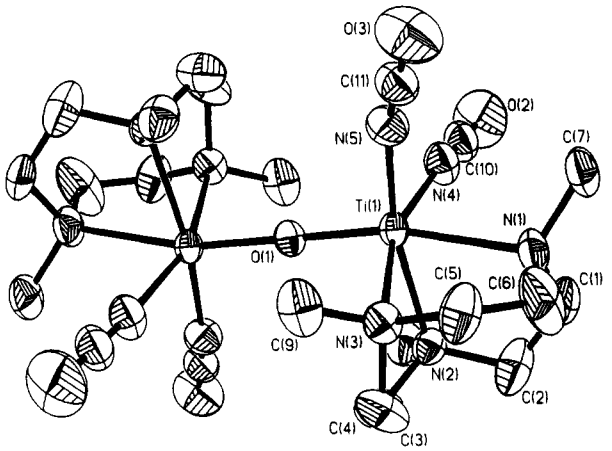

Figure 7. Structure of the neutral molecule in crystals of **4**.

Table 6. Atomic Coordinates ($\times 10^4$) and Equivalent Isotropic Displacement Parameters ($Å^2 \times 10^3$)

atom	*x*	*y*	*z*	*U*(eq)[a]
Ti(1)	6367(1)	5156(1)	5383(1)	37(1)
N(1)	8008(3)	5716(4)	5891(3)	57(2)
N(2)	5909(4)	6341(3)	6229(3)	47(2)
N(3)	6734(3)	6426(3)	4604(3)	49(2)
C(1)	7723(6)	6107(6)	6717(5)	98(3)
C(2)	6786(5)	6698(6)	6732(4)	82(3)
C(3)	5498(6)	7047(5)	5659(4)	79(3)
C(4)	6196(5)	7252(5)	4982(5)	76(3)
C(5)	7909(4)	6573(5)	4580(4)	71(2)
C(6)	8438(5)	6446(6)	5359(6)	113(4)
C(7)	8803(4)	4975(5)	6015(4)	71(3)
C(8)	5005(5)	6065(4)	6776(3)	64(2)
C(9)	6361(5)	6291(5)	3749(3)	68(2)
O(1)	5000	5000	5000	40(2)
N(4)	6432(4)	4183(4)	6332(3)	60(2)
C(10)	6312(5)	3742(5)	6905(4)	63(2)
O(2)	6199(5)	3273(4)	7505(3)	122(3)
N(5)	7219(3)	4327(3)	4576(3)	59(2)
C(11)	7871(5)	4150(5)	4105(4)	58(2)
O(3)	8571(4)	3955(4)	3616(3)	97(2)

[a] Equivalent isotropic U defined as one-third of the trace of the orthogonalized U_{ij} tensor.

Table 7. Selected Bond Distances (Å) and Angles (deg) for $[(Me_3tacn)_2Ti_2(NCO)_4(\mu\text{-}O)]$

Ti(1)–N(1)	2.360(5)	Ti(1)–O(1)	1.838(1)
Ti(1)–N(2)	2.269(5)	Ti(1)–N(4)	2.092(5)
Ti(1)–N(3)	2.274(5)	Ti(1)–N(5)	2.075(5)
N(5)–C(11)	1.152(8)	C(11)–O(3)	1.220(8)
N(4)–C(10)	1.143(9)	C(10)–O(2)	1.199(9)
N(1)–Ti(1)–N(2)	75.5(2)	N(1)–Ti(1)–N(3)	75.4(2)
N(2)–Ti(1)–N(3)	77.9(2)	N(1)–Ti(1)–O(1)	166.9(1)
N(2)–Ti(1)–O(1)	93.7(1)	N(3)–Ti(1)–O(1)	95.5(1)
N(1)–Ti(1)–N(4)	86.2(2)	N(2)–Ti(1)–N(4)	93.4(2)
N(3)–Ti(1)–N(4)	161.0(2)	O(1)–Ti(1)–N(4)	102.0(1)
N(1)–Ti(1)–N(5)	88.4(2)	N(2)–Ti(1)–N(5)	161.8(2)
N(3)–Ti(1)–N(5)	90.0(2)	O(1)–Ti(1)–N(5)	101.1(1)
N(4)–Ti(1)–N(5)	93.9(2)	Ti(1)–O(1)–Ti(1A)	180.0(1)
Ti(1)–N(4)–C(10)	167.4(5)	N(4)–C(10)–O(2)	179.1(7)
Ti(1)–N(5)–C(11)	156.6(5)	N(5)–C(11)–O(3)	179.0(7)

and an oxygen atom of the μ_2-oxo bridge. The Ti–O_{oxo} bond distance of 1.838(1) Å indicates some double bond character. It is somewhat longer than those in the crystallographically characterized linear (μ-oxo)dititanium(III) complex $[\{Ti(py)_3Br_2\}_2(\mu\text{-}O)]\cdot 2py$ (py = pyridine)[8a] with Ti–O_{oxo} distances of 1.794 and 1.798 Å. In the organometallic species $[\{Cp_2Ti\}_2(\mu\text{-}O)]$, the Ti–$O_{oxo}$ distance is also 1.838(1) Å and the Ti–O–Ti bond angle is slightly bent at 170.9(4)°.[8b] The oxo bridge in **4** exerts a pronounced structural trans influence on the Ti–N bond in trans position to the bridge as is clearly indicated by the difference of 0.088 Å between the Ti–N distances in trans and cis position relative to the oxo bridge. Table 8 gives a comparison of structural details of crystallographically characterized (μ-oxo)dimetal(III) species with trivalent first-row transition metals as a function of the respective d^n electron configuration.

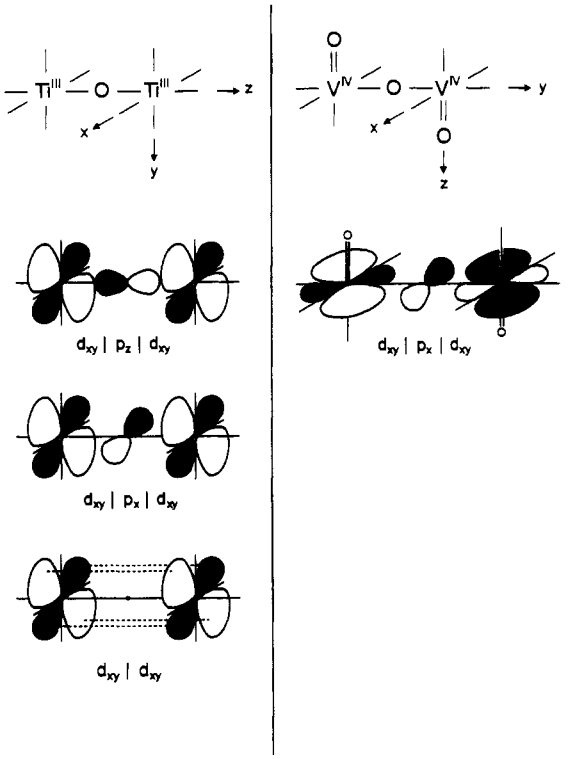

Figure 8. Orbital interactions in dinuclear complexes containing a $[Ti^{III}\text{–}O\text{–}Ti^{III}]^{4+}$ and a *trans*-$[OV^{IV}\text{–}O\text{–}V^{IV}O]^{2+}$ core.

Discussion

The most salient feature of the present work is the discovery of a weak antiferromagnetic coupling of the two d^1d^1 electrons in the linearly oxo bridged dititanium(III) complexes **4** and **5**. In the following we interpret this observation in the frame of the Goodenough–Kanamori rules for magnetic superexchange as they have been elegantly and clearly outlined in Ginsberg's 1971 review article.[1b]

We will use the coordinate system as defined in Figure 8. In complexes **4** and **5** the Ti–O_{oxo} bonds are the shortest; the titanium(III) ions have a $(d_{xy})^1$ electron configuration. It is then obvious that the following orbital interactions between the half-filled d_{xy} orbitals of the two titanium(III) ions and the filled p_x, p_y, p_z orbitals of the oxo bridge lead to ferromagnetic contributions because the magnetic orbitals are orthogonal: $d_{xy}|p_z|d_{xy}$; $d_{xy}|p_y|d_{xy}$; $d_{xy}|p_x|d_{xy}$. This simple analysis clearly shows that a linear oxo bridge in $Ti^{III}\text{–}O\text{–}Ti^{III}$ complexes cannot bring about an antiferromagnetic coupling; only ferromagnetic pathways exist. On the other hand, a direct through-space interaction between the two d_{xy} orbitals will result in spin pairing. Since the experimentally observed coupling is the sum of antiferromagnetic and ferromagnetic contributions, eq 3, it follows that in the present cases

$$J = J_{AF} + J_F \tag{3}$$

the direct $d_{xy}|d_{xy}$ interaction leads to a slightly larger value of J_{AF} than J_F. It is noted that at a Ti···Ti distance of 3.676 Å in **4** the direct overlap between the d_{xy} orbitals is probably quite small but it suffices to stabilize a diamagnetic ground state of the molecule. This model predicts a pronounced Ti–O–Ti angle dependence of the antiferromagnetic coupling. When the angle decreases, the Ti···Ti distance will decrease and the direct $d_{xy}|d_{xy}$ interaction will increase. Consequently, a larger J_{AF} contribution should be observed. This is indeed the case for complexes containing a

Table 8. Comparison of Representative Structural Data for (μ-Oxo)dimetal(III) Complexes

complex	$d^n d^n$	M–O_{oxo}, Å	M–O–M, deg	$\Delta[(M-N)_{trans} - (M-N)_{cis}]$,[a] Å	ref
$[\{LTi(NCO)_2\}_2(\mu\text{-}O)]$	d^1d^1	1.838(1)	180	0.088	this work
$[\{Ti(py)_3Br_2\}_2(\mu\text{-}O)]\cdot 2py$	d^1d^1	1.794, 1.798	180	0.05	8a
$[\{LV(acac)\}_2(\mu\text{-}O)]I_2\cdot 2H_2O$	d^2d^2	1.806(1)	180	0.10	5a
$[\{VCl(bpy)_2\}_2(\mu\text{-}O)]Cl_2\cdot 6H_2O$	d^2d^2	1.787(1)	180	0.054	5c
$[\{LCr(acac)\}_2(\mu\text{-}O)](PF_6)_2$	d^3d^3	1.795(3)	166.2(2)	0.050	15
$[Mn_2(5\text{-}NO_2saldien)_2(\mu\text{-}O)]$	d^4d^4	1.757(4), 1.751(4)	168.4(2)		4a
$[Mn_2(HB(3,5\text{-}iPr_2pz)_3)_2(\mu\text{-}O)]$	d^4d^4	1.77(1)	174.9(7)	–0.21	4b
$[\{L'Fe(acac)\}_2(\mu\text{-}O)](ClO_4)_2$	d^5d^5	1.782(5), 1.792(4)	158.6(3)	0.066	16

[a] Average difference between the metal–nitrogen bond distances in trans position to the M–O_{oxo} bond and of those in cis position. Abbreviations: L = 1,4,7-trimethyl-1,4,7-triazacyclononane; py = pyridine; acac = pentane-2,4-dionate; bpy = 2,2′-bipyridine; L′ = 1,4,7-triazacyclononane; 5-NO_2saldien = *N*,*N*′-bis(5-nitrosalicylidene)-1,7-diamino-3-azapentane; [HB(3,5-$iPr_2pz)_3$] = tris(3,5-diisopropylpyrazolyl)borate.

(μ-oxo)bis(μ-carboxylato)dititanium(III) core where the Ti–O_{oxo} distances are the same as in **4** but the Ti–O–Ti angle is 123°. These complexes are diamagnetic at room temperature;[18] they contain a weak Ti–Ti single bond (Ti···Ti 3.198 Å).

The validity of this model rests of course entirely on the assumption of a d^1_{xy} ground state at both Ti(III) ions. Low-symmetry components allow the admixture of other d orbitals into the ground state, and these in turn could give rise to the observed weak antiferromagnetic coupling. It is at present not possible to distinguish between these two mechanisms.

Toftlund's dinuclear vanadyl complex $[\{(tpa)VO\}_2(\mu\text{-}O)](ClO_4)_2$ where tpa represents the tetradentate ligand tris(2-pyridylmethyl)amine which has a *trans*-$[OV\text{–}O\text{–}VO]^{2+}$ core as depicted schematically in Figure 8 is also a well characterized example for two first-row transition metal ions with d^1 electronic configuration coupled by an oxo bridge. The terminal V=O distance at 1.62 Å is shorter than the V–O_{bridge} bond at 1.804 Å. Using the coordinate system in Figure 8 the unpaired electron is in a d_{xy} orbital (note the change of coordinates on going from the Ti^{III}_2 to the V^{IV}_2 dinuclear species in Figure 8). The $d_{xy}|p_x|d_{xy}$ interaction now provides a strong antiferromagnetic π-superexchange pathway. In agreement with this interpretation Toftlund's complex is nearly diamagnetic at room temperature.

Acknowledgment. We thank Professor A. X. Trautwein, Dr. E. Bill, and Diplom Physiker C. Butzlaff (Medizinische Universität Lübeck) for recording the ESR spectra and the magnetic susceptibility data. Financial support of this work by the Fonds der Chemischen Industrie is also gratefully acknowledged.

Supplementary Material Available: Tables listing details of the crystal data collection, anisotropic thermal parameters, positional parameters for the hydrogen atoms, distances, and angles (7 pages). Ordering information is given on any current masthead page.

(18) Bodner, A.; Drueke, S.; Wieghardt, K.; Nuber, B.; Weiss, J. *Angew. Chem.* **1990**, *102*, 60; *Angew. Chem., Int. Ed. Engl.* **1990**, *29*, 68.